Taylor & Francis
Taylor & Francis Group

Applied Artificial Intelligence
An International Journal

ISSN: (Print) (Online) Journal homepage: https://www.tandfonline.com/loi/uaai20

Biogeography-based Optimization of Artificial Neural Network (BBO-ANN) for Solar Radiation Forecasting

Ajay Kumar Bansal, Virendra Swaroop Sangtani, Pankaj Dadheech, Nagender Aneja & Umar Yahya

To cite this article: Ajay Kumar Bansal, Virendra Swaroop Sangtani, Pankaj Dadheech, Nagender Aneja & Umar Yahya (2023) Biogeography-based Optimization of Artificial Neural Network (BBO-ANN) for Solar Radiation Forecasting, Applied Artificial Intelligence, 37:1, 2166705, DOI: 10.1080/08839514.2023.2166705

To link to this article: https://doi.org/10.1080/08839514.2023.2166705

Published online: 30 Jan 2023.

APPLIED ARTIFICIAL INTELLIGENCE
2023, VOL. 37, NO. 1, e2166705 (334 pages)
https://doi.org/10.1080/08839514.2023.2166705

Taylor & Francis
Taylor & Francis Group

Biogeography-based Optimization of Artificial Neural Network (BBO-ANN) for Solar Radiation Forecasting

Ajay Kumar Bansal[a], Virendra Swaroop Sangtani[b], Pankaj Dadheech[c], Nagender Aneja[d], and Umar Yahya[e]

[a]Department of Electrical Engineering, Central University of Haryana, Mahendergarh, Haryana, India; [b]Department of Electrical Engineering, Swami Keshvanand Institute of Technology, Management and Gramothan, Jaipur, Rajasthan, India; [c]Department of Computer Science and Engineering, Swami Keshvanand Institute of Technology, Management and Gramothan, Jaipur, Rajasthan, India; [d]School of Digital Science, Univerisiti Brunei Darussalam, Darussalam, Brunei; [e]Department of Computer Science and Information Technology, Faculty of Science, Islamic University in Uganda, Kampala, Uganda

ABSTRACT

Renewable energy can help India's economy and society. Solar energy is everywhere and can be used anywhere, making it popular. Solar energy's drawbacks are weather and environmental dependencies and solar radiation variations. Solar Radiation Forecasting (SRF) reduces this drawback. SRF eliminates solar power generation variations, grid overvoltage, reverse current, and islanding. Short-term solar radiation forecasts improve photovoltaic (PV) power generation and grid connection. Previous promising SRF studies often fail to generalize to new data. A biogeography-based optimization artificial neural network (BBO-ANN) model for SRF is proposed in this work. 5-year and 6-year data are used to train and validate the model. The data was collected from India's Jaipur Rajasthan weather station from 2014 to 2019. This work used biogeography-based optimization (BBO) to optimize and adjust the inertia weight of artificial neural networks (ANN) during training. The BBO-ANN model developed in this study had a Mean Absolute Percentage Error (MAPE) of 3.55%, which is promising compared to previous SRF studies. The BBO-ANN SRF model introduced in this work can generalize well to new data because it was able to produce equally accurate autumn and winter forecasts despite the great climatic variation that occurs during the summer and spring.

ARTICLE HISTORY
Received 21 June 2022
Revised 21 December 2022
Accepted 4 January 2023

Introduction

Because people are becoming more aware of the environment, steps have been taken to reduce the bad effects of traditional energy production methods and increase the use of renewable energy sources. Renewable energy research is growing because fossil fuels are running out and people want clean, green energy (Ajayi et al. 2014). It is essential to discover alternative energy sources with low ecological effect (Benmouiza and Cheknane 2019). By adding

CONTACT Umar Yahya umar.yahya@iuiu.ac.ug Department of Computer Science and Information Technology, Faculty of Science, Islamic University in Uganda, Kampala, Uganda

renewable energy sources to the power system, users can get high-quality, reliable electricity at an affordable price (Khare, Nema, and Baredar 2016; Marquez and Coimbra 2011).

The amount of sunlight that reaches the Earth's surface is affected by factors like latitude, altitude, and climatic conditions Guermoui et al. (2020). However, forecasting solar radiation requires knowledge of climatic variables such as solar irradiance, air temperature, wind speed and direction, atmospheric pressure, humidity, and cloud cover. Solar radiation forecasting is thus challenging. Obtaining precise demand and supply figures is essential for a grid operator. The electricity grid operators have a tough time adjusting for power shortages and surpluses caused by the use of traditional energy sources. A more assured grid is maintained with the help of accurate solar radiation forecasts, which also improves system reliability, maintains power quality, reduces the need for massive backups of energy storage, and increases the penetration of solar-powered systems. Solar radiation forecasting has a wide range of potential uses, depending on the time frame considered.

To better integrate solar photovoltaic (Solar PV) systems into the existing grid; to more accurately track the daily load; and to ensure that owners of solar photovoltaic power plants can more easily enter the market and raise their income, researchers have spent the past decade conducting extensive research on solar radiation forecasting. Solar energy systems provide energy that is secure, independent, and location-based. Solar energy systems give you the energy that is safe, free, and based on your location. Solar energy systems are used by many people and help the economy grow (Dinpashoh et al. 2019). The biggest problem with solar energy systems is that they are unstable and primarily depend on the prevailing weather and climate. Because of how these factors affect the performance of a single source system, its source equipment must be made bigger (López, Batlles, and Tovar-Pescador 2005). Consequently, incorporating renewable energy sources into the system requires weather forecasting (Marquez and Coimbra 2011). Darkness, cloudy weather, and rain make it hard to use solar energy. This is similar to the case of Wind energy, where wind turbines cannot work if there is no wind or if there is too much (i.e., hurricanes). For renewable energy and grid performance to be at their best, reliable forecasting methods are needed (Guermoui et al. 2020; Peled and Appelbaum 2013).

Previous scientific studies on empirical, statistical, machine learning, and satellite-based ways to estimate solar radiation (Mohanty, Patra, and Sahoo 2016). Most research done today uses hybrid models to predict solar radiation. Generally, the methods are characterized as empirical methods (Allen et al. 2005; Prescott 1940; Rensheng et al. 2004; Wu, Liu, and Wang 2007; Zhao, Zeng, and Han 2013), statistical approach (David et al. 2016; Ghimire et al. 2019; Jiang 2008; Shamshirband et al. 2016), machine learning techniques based methods (Benghanem, Mellit, and Alamri 2009; López, Batlles, and

Tovar-Pescador 2005; Voyant et al. 2017), and satellite-based methods (Allen et al. 2005; Feng et al. 2018; Pinker, Frouin, and Li 1995; Samani et al. 2007). While promising forecasting models have been reported in previous studies, it is worthy appreciating the continued need for better forecast models that are able to generalize to new data.

Artificial Neural Network (ANN) is a popular AI-based technique due to its ease of implementation as well as its effectiveness in handling nonlinear data. The input variables, weight combinations, architecture, and training procedure are the primary determinants of an ANN's performance. ANN is a great way to forecast events in time series data because it is based on the relationship between the input and output data sets. The training process affects ANN's performance, and it can understand complex, nonlinear interactions (Premalatha and Valan Arasu 2016). ANN is made by first figuring out the inputs, designing the network structure, learning about the network, and then using the learned ANN to make forecasts or predictions of the correct outputs. Non-linear forecasting or prediction is used to predict meteorological parameters (such as temperature, humidity, wind speed, solar radiations, etc.) at different time scales (hourly, daily, and monthly). The ability of ANN to learn and generalize depending on its application makes it a significant method. However, training neural networks is challenging and requires much computational time (Antonopoulos et al. 2019).

Even though it takes a long to converge, the back-propagation training algorithm is the most popular way to train ANN (Jiang 2008). Building ANN and choosing which ones to use is a complex optimization problem. Some researchers have examined the optimization strategies for choosing the right structure, training algorithm, transfer learning, and tuning hyperparameters based on training data (Renno, Petito, and Gatto 2016). Due to its gradient-based learning method, a back-propagation-based neural network (BPNN) works slowly and takes a long time to train (Khan and Sahai 2012). Using bio-inspired training approaches may significantly improve the training phase of ANN-based models, resulting in more precise and quick estimates (Yaghini, Khoshraftar, and Fallahi 2013; Zhao, Zeng, and Han 2013). Recent research has used soft computing approaches for ANN training and structural optimization (Yadav and Chandel 2014).

Various ANN based methods (Yadav and Chandel 2014), such as the multi-nonlinear regression algorithm (Ozgoren, Bilgili, and Sahin 2012), radial basis function techniques (Hejase, Al-Shamisi, and Assi 2014), kernel extreme learning machine model (Shamshirband et al. 2015), NN-ARX method (Shamshirband et al. 2016), adaptive neuro-fuzzy inference system, Elman recurrent network, feed-forward neural network (Sfetsos and Coonick 2000), wavelet neural network (Sharma et al. 2016), transform K-means (Azimi, Ghayekhloo, and Ghofrani 2016), long short-term memory model (Abdel-

Nasser and Mahmoud 2019; Srivastava and Lessmann 2018) have been presented for projecting sun radiation at various sites.

Most previous efforts in solar radiation forecasting have focused on building models on a single time scale. Therefore, additional research into solar radiation forecasting that takes into account a variety of scales is required. Since the new energy sector has more stringent criteria for forecasting speed, intelligence, accuracy, controllability, and planning. This paper's main contribution is the proposal of a solar radiation forecasting (SRF) model which addresses the common forecast problems of being able to achieve accurate short- to medium-term solar radiation forecasts, particularly when dealing with a vast disparity in time scales.

In this research, a new technique utilizing biogeography-based optimization ANN (BBO-ANN) is built to forecast solar radiation using meteorological station data from India's Jaipur weather station. The data was gathered using sun radiation measurements. The performance of the BBO-ANN SRF model built in this work is evaluated and resulted compared with previous SRF models in literature.

Methods

Artificial Neural Network

Several neurons or nodes are connected systematically to create an artificial neural network (ANN) inspired by the human brain. Nevertheless, neurons in an ANN use mathematical functions. There are three layers: input, hidden, and output. It processes both inputs to hidden layers and hidden to output layers through weighted synaptic connections. If the neural network has more than one hidden layer, they have additional connection weights. During the training phase, the connection weights are changed to reduce the variance between the desired and actual output. The neural network uses the training data to learn the relationship between input and output and improve its performance. A multi-layer feed-forward neural network, as seen in Figure 1, is the neural network topology most often used for time series forecasting.

The neural network structure for each given application is determined by simulating many possible combinations and then applying the input-output data set. The problem definition serves as the inspiration for the network structure. The training procedure is very reliant on the training data set. The data set is divided into training, validation, and testing. Training set information is used to change the weights, validation set information is used to verify the network performance, and testing set information is used to test the network performance.

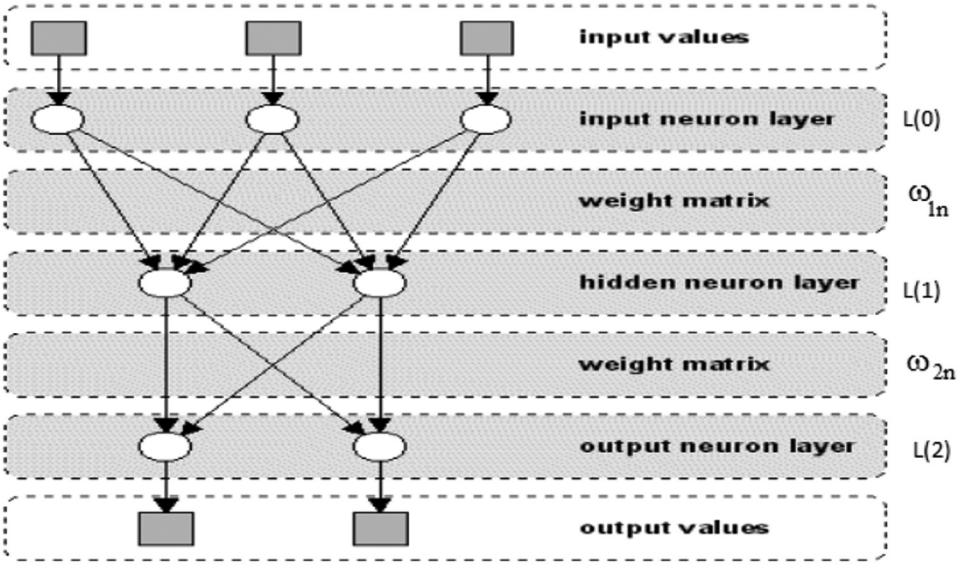

Figure 1. A simple three-layer feed-forward neural network.

Biogeography-Based Optimization

A biogeography-based optimization method was developed by (Simon 2008). Biogeography-based optimization (BBO) is a blend of bio-inspired optimization and population-based evolutionary algorithm (EA) (Bansal and Garg 2021). Biogeography is the study of species' behavior in nature concerning time and distance, as well as the movement of species across environments. The population combines tentative solutions generated by the BBO algorithm, represented as a vector of numbers (Mandal et al. 2011). The BBO algorithm uses the migration operator to facilitate the transfer of information across solutions. The adaptable qualities of the BBO algorithm promote its use for resolving complicated optimum sizing problems involving hybrid energy systems.

The notion of biogeography stipulates that organisms migrate from one island to another based on various conditions. It also investigates how species evolve and go extinct. In biogeography, habitats are biological regions that are not directly linked to other regions and are inhabited by specific plant and animal species. Each habitat is defined by its habitat suitability index (HSI) parameter. A habitat is a likely solution to the problem. A high HSI indicates the presence of a large number of species, while a low HSI indicates the presence of a limited number of species. The appropriateness of the region determines species-specific habitat quality. HSI is shown as a function of the values of characteristics that determine habitability and are often referred to as "Suitability Index Variables" (SIV). As it is readily apparent, HSI is a dependent variable, while SIV is an independent variable.

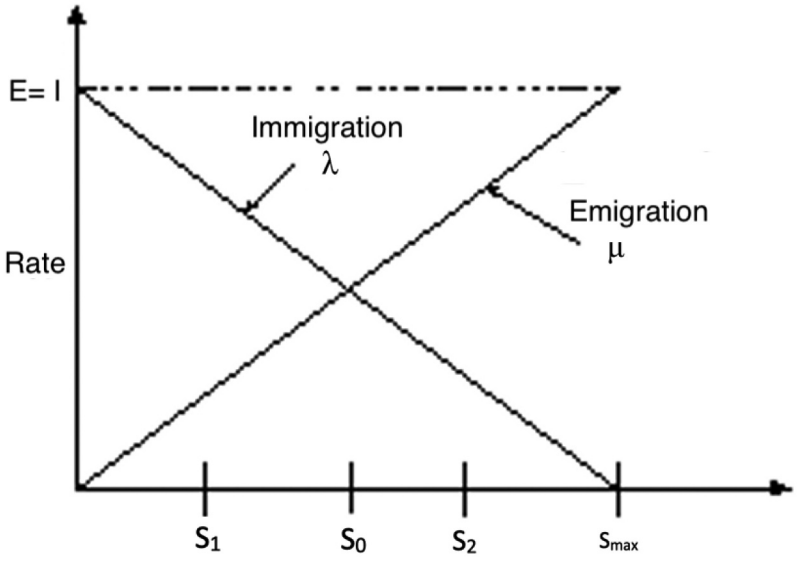

Figure 2. Biogeography model of immigration rate and emigration rate.

High HIS environments have a high emigration rate μ and a low immigration rate λ due to species saturation (Rahmati and Zandieh 2012). If other ecological circumstances are suitable, HSI may increase in low-HSI settings. If a habitat's HIS remains low throughout the iterative process, the immigration rate will climb. Habitat HSI, immigration rate, and emigration rate are considered to be linearly related.

Figure 2 illustrates the correlations among the number of species, the emigration rate μ, and the immigration rate λ. S indicates the number of species in a habitat, indicating the environment's fitness. Maximum species in a habitat is denoted by S_{max}, while S_0 denotes the circumstance when emigration rate equals immigration rate. From Figure 2, we may deduce that the island with the best performance (S_2) has a large μ and a small λ, and vice versa. After analyzing HSI of each solution Hk, λk and μk are evaluated by Equations 1 and 2, respectively. A high-HIS environment has a high μk and a low λk because species in high-HSI habitats tend to move to low-HSI habitats (Singh and Kamal 2012)

$$\lambda_i = \frac{EK}{P}, \text{where Eis maximum emigration rate} \tag{1}$$

$$\mu_i = I - \left(1 - \frac{K}{P}\right) \text{where Iis maximum immigration rate} \tag{2}$$

HSI is the objective function during optimization, and the habitat with the highest HSI is chosen.

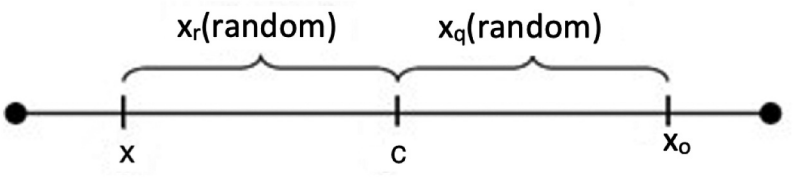

Figure 3. Opposition-based learning members.

Oppositional BBO

Opposition-based learning (OBL) is used in EAs to accelerate convergence. In OBL, convergence speed is increased by maintaining high-fitness individuals or their opposites. The opposite is the replication of any individual across the search space midpoint. Figure 3 illustrates, for each population member *x*, there are three opposing members, opposite *xo*, quasi-opposite *xq*, and quasi-reflected opposite *xr* across the center of the domain point *c*. *xo* is a replica of *x* across *c*, *xq* is a random replica point between *xo* and *c*, and *xr* is a random replica point between *x* and *c*.

OBL is more efficient than random mutations since it is an intelligent algorithm. It is evident that the quasi-opposite number *xr* is closer than *x*, *xq*, and *xo*. To facilitate understanding, the population size is assumed to be *N*, and OBBO generates *N* opposite individuals. Among the 2*N* individuals that comprise the next population, the top *N* individuals survive. The OBL approach is not processed at each step, but rather with a probability *jr*, also known as the jump rate. In each iteration of the OBBO algorithm, the initial *N* individuals of the population are preserved. Based on the jump rate, the opposing population of *N* individuals is then produced. Now, the best *N* individuals out of a total of 2*N*, 3*N*, or 4*N* are chosen for the following generation. This strategy guarantees that every person will be at least as excellent as the previous one.

Solar Radiation Components Important to SRF

Solar radiation indicates the amount of the sun's energy reaching the earth's surface via the atmosphere at a given moment. There are two components to solar radiation: beam radiation and diffuse radiation. Beam solar radiation is the radiation that travels down the line connecting the surface to the sun. Diffuse solar radiation is radiation that cannot reach the surface due to air obstructions. If diffuse solar radiation is less than or equal to 25% of total solar radiation, the sky is considered clear. A standard "clear sky" condition is used for solar radiation forecasting, and total solar radiation is computed under cloudless circumstances. Long-term average meteorological data are necessary

for accurately predicting solar radiation under a clear sky. Long-term meteorological data collecting is a complex and time-consuming endeavor.

Designing hybrid energy systems requires knowledge of the total solar radiation in a given location. With the increased usage of solar energy and the integration of solar energy into the power system, effective modeling and forecasting techniques are required. Solar radiation forecasting is required for the development and performance estimation of solar energy devices. Solar radiation is very crucial for power plant operation planning. The objective of the proposed study is to examine ANN utilizing Jaipur's vast range of solar radiation data under clear skies.

ANN Structure Implementation

ANN input parameters include latitude, longitude, month, day, time of day, an elevation of the field site season, and solar radiation data from the past 48 instances. As training data, we utilize the measured data spanning five years, from January 1, 2014, to December 31, 2018.

The trained network is validated using data from January 1, 2019, to December 31, 2019 (Figure 4). Figure 5 shows a sample of the hourly sun radiations recorded for Jaipur (Rajasthan) over a year. During network training, the circulate approach is used, whereby each training data set moves the input vector and target vector from the first week to the next hour of the following week. During training, hidden layers are learned, and their weights are adjusted depending on input-output errors. The relu and sigmoid activation functions are employed in the hidden and output layers. The activation functions are chosen via a system of trial and error. A neural network modifies weights depending on the deviation between expected and desired outputs. Solar radiations are measured hourly for a whole year in Jaipur (Rajasthan), as shown in Figure 6. Each training data set shifts the data from the first week as the input vector and the data

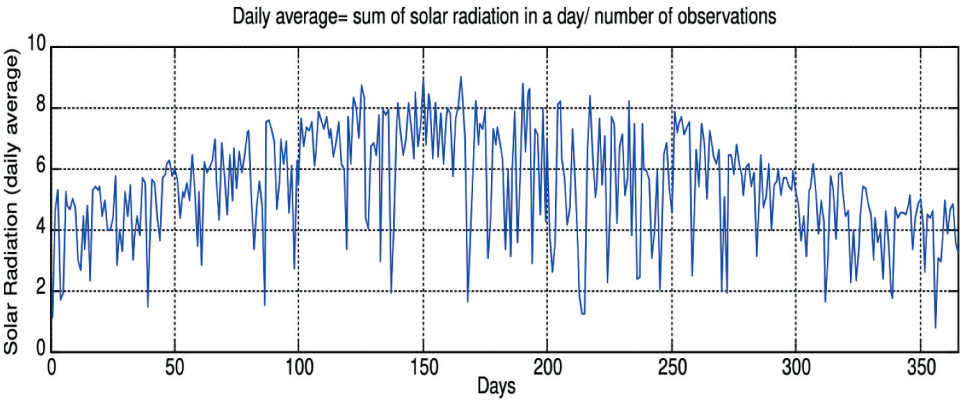

Figure 4. Typical average daily solar radiation (kW/m2) for Jaipur (Rajasthan).

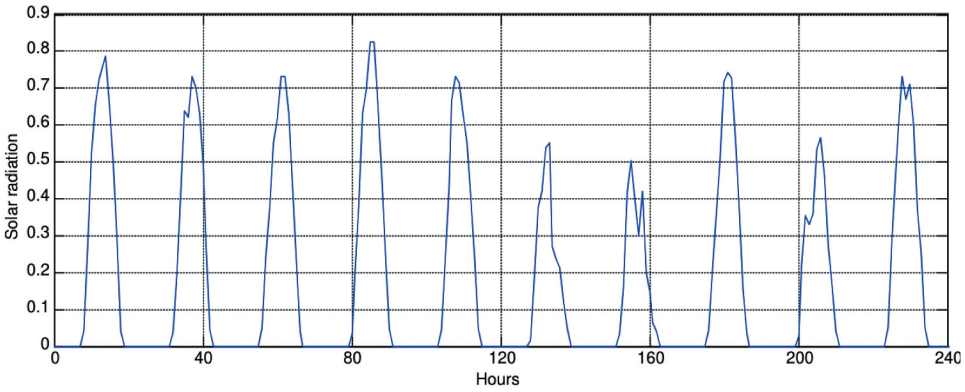

Figure 5. Hourly solar radiation (kW/m2) pattern for Jaipur (Rajasthan).

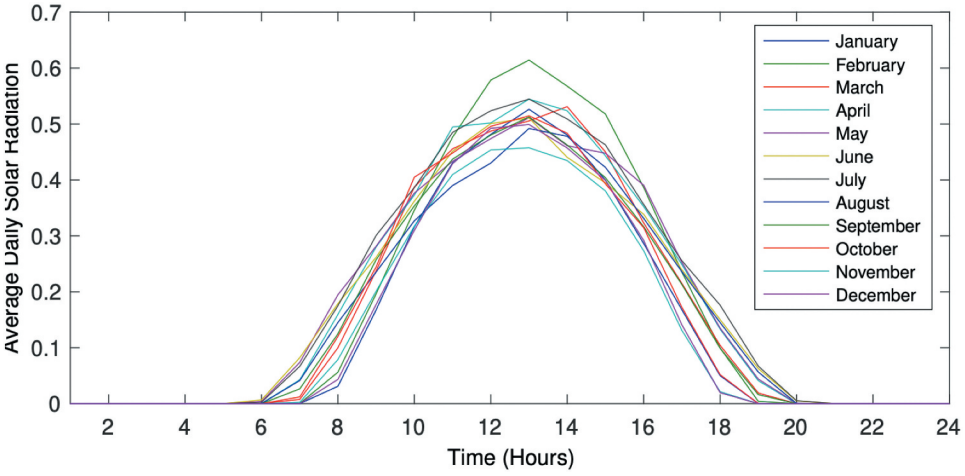

Figure 6. Hourly solar radiation (kW/m2) pattern for Jaipur (Rajasthan).

from the second week as the target vector to the following hour using the circulate technique.

After attempting many combinations, the ANN used to forecast solar radiation settles on having one input layer, one output layer, and two hidden layers. As can be seen in Table 1, the input variables are 55. The input layer comprises 55 nodes, and the output layer includes one node. As a result of trying several different permutations of hidden layer nodes and taking into account the complexity of the problem, the number of nodes in the first hidden layer is 36, and the number in the second hidden layer is 18. The ANN has arrived at its final structure, "55-36-18-1," as shown in Figure 7.

Table 1. Artificial neural network input parameters for solar radiation forecasting.

SN	Detail of variable	Number of inputs
1	Latitude	1
2	Longitude	1
3	Elevation of the field site	1
4	Season	1
5	Solar Radiation	48
6	Month	1
7	Day	1
8	Hour of the Day	1

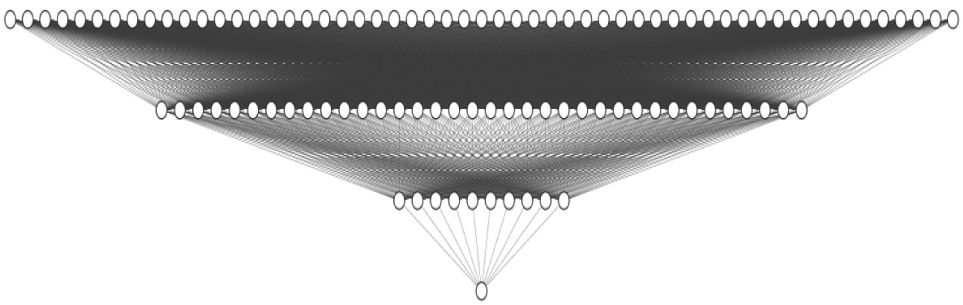

Figure 7. Ann – 55-36-18-1.

The BBO-ANN Implementation Algorithm

A downside of backward propagation for artificial neural networks (BPANN) is the potential for trapping at local minima and the slow pace of convergence. Basically, a hill climbing strategy may be used to understand BPANN learning. When the cost function is less than the local minimum in the weight space, the network might get stuck at that point. An ANN has several different parameters, including the quantity of input, hidden, and output nodes, learning rate, momentum rate, bias, minimal error, and activation/transfer function. The Particle Swarm Optimization (PSO) method is based on the social adaptation of knowledge, and all individuals are seen as belonging to the same generation. The genetic algorithm (GA) algorithm is based on evolution and does not account for changes within a single generation. The disadvantages of the PSO-based training approach include the fact that the selection of PSO parameters has a significant impact on network stability and performance. Incorrect parameter selection may result in premature convergence and erroneous simulation results.

In this paper, the BBOANN is proposed, the suggested training method optimizes the training process by increasing convergence speed and the likelihood of finding a suitable application solution. As described in Algorithm 1, the BBOANN method has two key parts: the first is the Neural Network prediction phase, in which the ANN performance is assessed using the set of weights chosen. The second section is an OBBO method for modifying the

Algorithm 1 Pseudo code of BBO based ANN training

```
Initialize ANN configuration
Initialize the population
Assign weights (habitats) to ANN
Evaluate ANN mean square error and equate these as individual's fitness
for 1 to number of iterations do
    Generate opposite population
    Set emigration and immigration probability based on fitness
    for 1 to size of population do
        Evaluate each individual's fitness as ANN mean square error
        if habitat is selected probabilistically based on immigration rate then
                                                          ▷ Migration operation
            Randomly select SIV from habitat
            Replace random SIV in habitat
        if habitat is selected probabilistically based on jumping rate then
            Generate quasi-reflected opposite population
    Implement elitism by replacing and removing bottom habitat
Return solution with best fitness
```

ANN weights based on the first section's evaluation of the ANN's performance.

The BBO-ANN Training and Validation Process

The processes involved in designing the ANN model included the following steps:

(1) Normalize the input and target values.
(2) Partition the dataset for training and validation purposes. This required setting the size of the input matrices and generating training and validation datasets.
(3) Create a multilayer feed-forward neural network as described above in Figure 7.
(4) A training method updates network weights to minimize the network performance function (called Mean Square Error). BPANN, GAANN, PSOANN, and BBOANN are utilized for training.
(5) After the ANN was trained, the target output was predicted using the input data.
(6) In order to calculate the actual predicted value, the output that was obtained in step 5 is unnormalized.

The first eighty-five percent of the input data from each period were roughly provided to the network for training purposes. During training, the weight/bias matrix that is formed after the first data set is saved and later utilized as the starting point for the future training period. This procedure was repeated until all of the periods had been utilized in the subset, and the network weights and biases had been continuously adjusted from one period to the next. During training, the mean absolute percentage error (MAPE) between the

network's internal forecasts and the target values generally started very high but quickly dropped and settled near the MAPE minimum after about ten epochs. This occurred because the network was learning how to make accurate forecasts. The mean absolute percentage error minima are in the single digits, indicating that the network outputs closely fit the training data. In most cases, MAPE started high (around 100) but rapidly decreased to its lowest point (around 2) during the training session.

250 predictions are produced for each period in the subset during testing using the network that was trained during the development phase. The neural network predictions were contrasted with the competing forecast values derived from a distribution with a climatological basis. Persistence forecasting assumed that all predicted valid times and the hourly average solar radiation would be the same at the projected start time. Mean Absolute Error, Mean Squared Error, and Maximum Error was calculated as the indicators of prediction performance for the neural network and each of the forecast alternatives. These errors are disparities between predicted and actual solar radiation.

Evaluation of the BBO-ANN Trained SRF Model

Various criteria are used to assess the solar radiation forecasting algorithms' accuracy. The performance of forecasting techniques is assessed using the Mean Absolute Percentage Error (MAPE), Root Mean Square Error (RMSE), Normalized Root Mean Square Error (nRMSE), and Mean Bias Error (MBE) criteria.

$$RMSE = \sqrt{\frac{1}{N}\sum_{n=1}^{N}\left[\hat{S}(n) - S_{actual}(n)\right]^2} \tag{3}$$

$$nRMSE = \frac{\sqrt{\frac{1}{N}\sum_{n=1}^{N}\left[\hat{S}(n) - S_{actual}(n)\right]^2}}{\frac{1}{N}\sum_{n=1}^{N} S_{Actual}(n)} \tag{4}$$

$$MAPE = \frac{1}{N}\sum_{n=1}^{N}\left|\frac{\hat{S}(n) - S_{actual}(n)}{S_{actual}(n)}\right| \tag{5}$$

$$MBE = \frac{1}{N}\sum_{n=1}^{N}\hat{S}(n) - S_{actual}(n) \tag{6}$$

Results and Discussion

BBO-ANN

The weight vector of an ANN, with all of its biases, is represented by a population. Every population revises its position by computing new migration rates, which are then applied to moving individuals to the new location. For BBO, they continue to use the extra weights even though there has been no discernible improvement. Every population carries out this practice. For solar radiation forecasting, the developed BBOANN technique has been utilized in Jaipur, Rajasthan (India). The accuracy of the findings ranges from two to six percent during the course of the year, demonstrating the dependability of the suggested BBOANN. The numerical results obtained using the suggested BBOANN technique are shown in Figures 8, 9, 10, 11 for winter, spring, summer, and fall days.

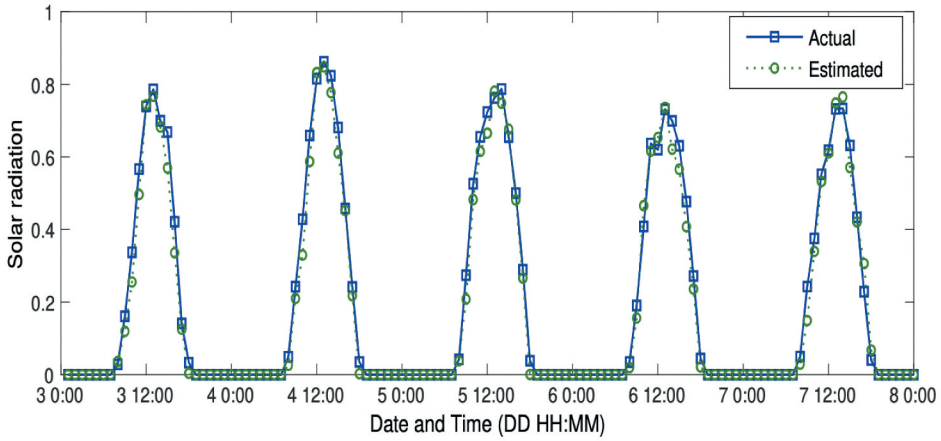

(a) Hourly Actual and forecasted solar radiation, in KW/m^2

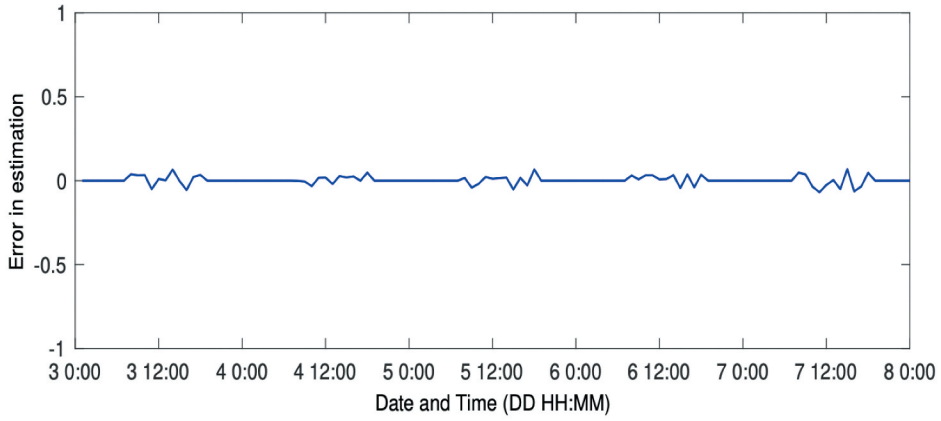

(b) Estimation error, in KW/m^2

Figure 8. BBOANN solar radiation forecasting winter season, Jan 3 to Jan 8, 2019.

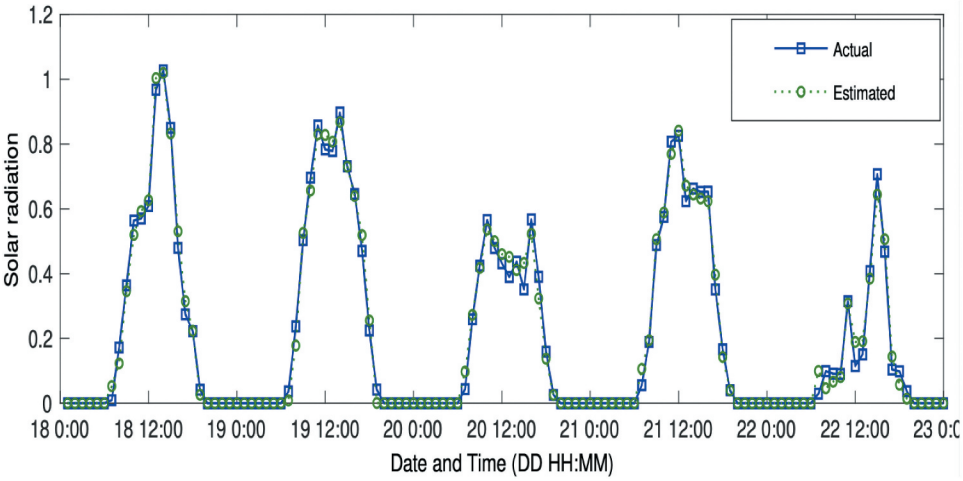

Figure 9. BBOANN solar radiation forecasting spring season Apr 18 to Apr 232,019 Hourly Actual and forecasted solar radiation, in KW/m^2.

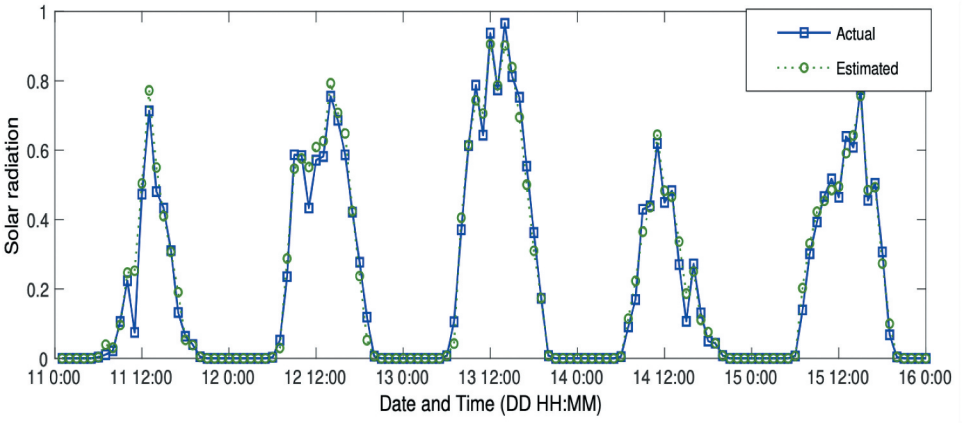

Figure 10. BBOANN solar radiation forecasting summer season, Jul 11 to Jul 162,019 Hourly Actual and forecasted solar radiation, in KW/m^2.

When using MATLAB 2020 on a PC with 8 GB of RAM and a 2.1 GHz-based CPU, the average calculation time for predicting a whole week is less than 1.4 seconds. The values for the criteria to assess the suitability of the suggested ANN technique in predicting solar radiation are shown in Tables 2 and 3. The season is shown in the first column, the MAPE in the second, the square root of the SSE in the third, and the SDE in the fourth.

Comparison of Solar Radiation Forecasting Methods

The findings show that all models have acceptable solar radiation forecasting accuracy for the winter, spring, summer, and autumn seasons. The forecasting

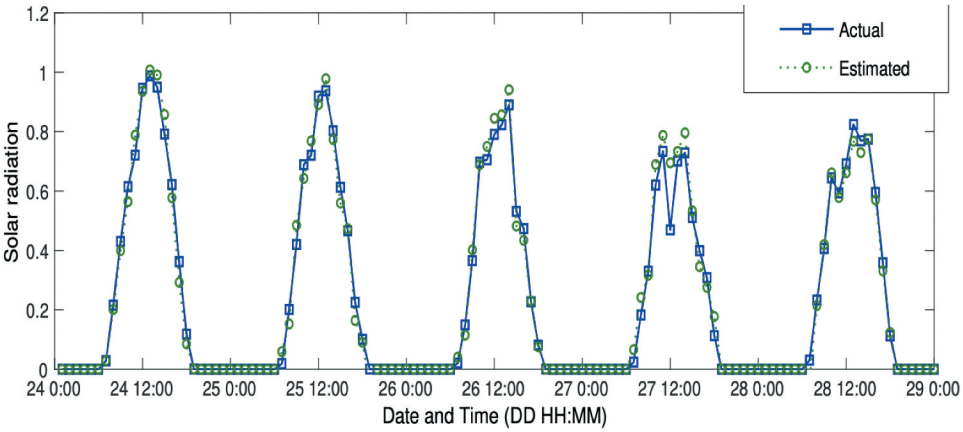

Figure 11. BBOANN solar radiation forecasting fall season, Oct. 24 to Oct. 29, 2019 Hourly Actual and forecasted solar radiation, in KW/m^2.

Table 2. Performance analysis of BBOANN solar radiation forecasting for 2019.

Season	MAPE (%)	MBE (W/m2)	RMSE (W/m2)	nRMSE (%)
Winter	2.98	47.4	48.2	10.5
Spring	2.01	42.9	54.3	10.1
Summer	3.14	29.6	36.8	8.47
Fall	3.41	36.8	43.2	8.98

Table 3. RMSE performance analysis of BBOANN solar radiation forecasting for 2019.

Algorithm	Jan	Feb	Mar	Apr	May	Jun	Jul	Aug	Sep	Oct	Nov	Dec
BPANN	67	124	87	164	123	96	92	89	102	121	112	78
GAANN	73	92	98	118	103	81	70	67	78	89	78	56
PSOANN	62	75	84	108	82	79	84	58	74	98	108	64
BBOANN	48	43	57	78	41	52	35	41	47	48	58	39

of solar radiation using artificial neural networks (ANN) is the main emphasis of this paper. The results are compared with Convolution Neural Network integrated with LSTM (CLSTM) proposed by (Huang et al. 2013), Radial Basis Function Neural Network (RBFNN) (Ren, Suganthan, and Srikanth 2015), Recurrent Neural Network (RNN) (Chaouachi, Kamel, and Nagasaka 2010), Clustered ANFIS network (Benmouiza and Cheknane 2019), and two common benchmark algorithm, clear-sky index persistence (CSpers) prescott1940evaporation, Elman neural network (ENN) prescott1940evaporation.

The proposed BBOANN, BPANN, GAANN, and PSOANN approaches are compared seasonally to RNN, RBFNN, CLSTM, and ENN in Table 4 for MAPE and RMSE. The average MAPE is 3.55% for the BBOANN, 3.97% for GAANN, 4.08% for PSOANN, 5.32% for BPANN, and 6.76% for RNN, 5.50% for RBFNN, 4.34% for CLSTM, and 6.57% for ENN. Figure 12 compares all four neural network types for predicting the sun radiation throughout the summer.

Table 4. Comparative MAPE (%) and RMSE (Wm-2) results of solar radiation forecasting methods on eight days.

		Winter		Spring		Summer		Fall	
Method	Error	Jan 3	Feb 7	Apr 18	May 2	Jul 11	Aug 5	Oct 24	Nov 8
BBOANN	MAPE	2.98	2.56	4.01	4.21	4.14	4.02	3.41	3.1
	RMSE	50.6	47.9	78.3	43.2	35.4	37.3	48.8	55.3
BPANN	MAPE	3.48	5.98	4.45	8.87	4.35	6.98	3.86	4.56
	RMSE	76.4	147.3	172.7	132.8	92.4	98.5	121.4	112.4
GAANN	MAPE	3.56	3.92	4.62	4.24	4.07	4.74	3.32	3.86
	RMSE	76.3	98.4	118.4	110.3	70.2	76.7	89.3	48.6
PSOANN	MAPE	3.42	3.57	4.28	4.01	4.19	4.78	3.63	3.86
	RMSE	64.2	65.5	72.3	77.1	64.1	68.4	78.4	88.2
RNN	MAPE	15.48	17.98	19.45	16.87	10.35	9.98	14.86	13.56
	RMSE	155.3	142.1	218.4	254.2	132.4	147.8	212.4	201.3
RBFNN	MAPE	12.56	15.92	16.62	12.24	8.07	8.74	11.62	10.86
	RMSE	194.8	172.5	153.4	143.7	142.3	132.9	98.3	173.2
CLSTM	MAPE	7.98	7.56	10.01	7.21	5.14	5.02	7.41	8.1
	RMSE	185.8	139.2	132.9	173	155.3	179.9	153.7	155.3
ENN	MAPE	5.53	7.39	8.34	10.87	5.35	6.23	5.74	7.33
	RMSE	154.3	189.6	216.4	156.3	136.8	124.5	207.4	187.3

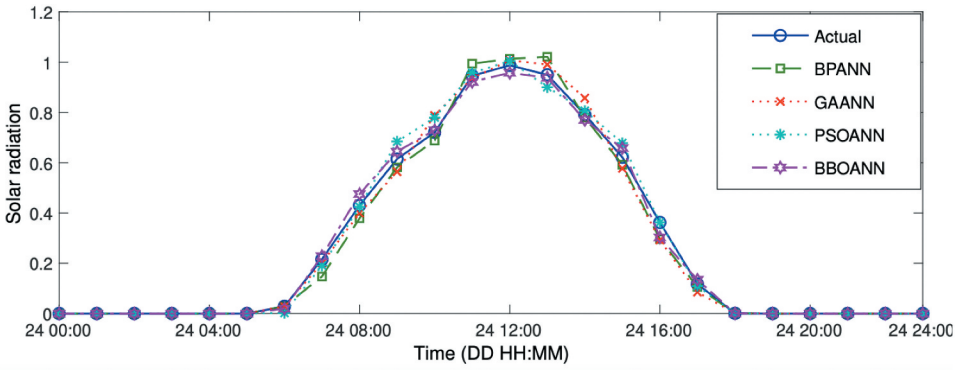

Figure 12. Comparison of neural networks of solar radiation forecasting Oct., 2019.

It is clear from Figure 13 that solar radiation forecasts for the autumn and winter months had the lowest mean absolute percentage error (MAPE) of any approach. The MAPE readings vary more throughout the summer and spring seasons since the weather is most variable during these times. The unpredictability of data patterns is the primary cause of MAPE variance throughout four seasons. The proposed BBOANN technique has the lowest MAPE overall, making it the most precise forecasting method.

The comparison of several approaches shows that no one algorithm is superior, with lowest MAPE values year-round. The choice of starting weights has an impact on performance and the search space of neural network training contains several local minima. The different optimization algorithms that draw inspiration from nature enhance the neural networks' capacity for search

Figure 13. Comparison of different solar radiation forecasting methods for MAPE and RMSE.

and forecasting accuracy. In particular, Table 2 makes it clear that accuracy is improved by combining an optimization technique with neural network.

Conclusion

Due to the non-linear relationship between input and output, predicting solar radiation is not a trivial problem. This non-linear characteristic favors the ANN-based techniques for forecasting solar radiation. In the current study, a biogeography-based optimization approach of the ANN technique is designed and put to use. With the use of MAPE, MBE, RMSE, and nRMSE, the performance of the BBO-ANN forecasting technique was evaluated. According to the findings, BBO-ANN produced the most precise and effective SRF models, whereas the regular ANN models underperformed compared to it. BBO-ANN model as it was able to forecast solar radiation for given inputs in just under two seconds. When BBO-ANN performance was compared to existing benchmark SRF methods and other techniques described in the literature, it was clear that the BBO-ANN SRF approach introduced in this work, was not only more accurate but also more efficient, computation-wise.

Disclosure statement

No potential conflict of interest was reported by the author(s).

ORCID

Umar Yahya http://orcid.org/0000-0002-4255-0364

References

Abdel-Nasser, M., and K. Mahmoud. 2019. Accurate photovoltaic power forecasting models using deep lstm-rnn. *Neural Computing & Applications* 31 (7):2727–40. doi:10.1007/s00521-017-3225-z.

Ajayi, O., O. Ohijeagbon, C. Nwadialo, and O. Olasope. 2014. New model to estimate daily global solar radiation over nigeria. *Sustainable Energy Technologies and Assessments* 5:28–36. doi:10.1016/j.seta.2013.11.001.

Allen, R. G., M. Tasumi, A. Morse, and R. Trezza. 2005. A Landsat-based energy balance and evapotranspiration model in western us water rights regulation and planning. *Irrigation and Drainage Systems* 19 (3):251–68. doi:10.1007/s10795-005-5187-z.

Antonopoulos, V. Z., D. M. Papamichail, V. G. Aschonitis, and A. V. Antonopoulos 2019. Solar radiation estimation methods using ann and empirical models. *Computers and Electronics in Agriculture 160*, 160–67.

Azimi, R., M. Ghayekhloo, and M. Ghofrani. 2016. A hybrid method based on a new clustering technique and multilayer perceptron neural networks for hourly solar radiation forecasting. *Energy Conversion and Management* 118:331–44. doi:10.1016/j.enconman.2016.04.009.

Bansal, A. K., and V. Garg (2021). Biogeography-based optimization (bbo) trained neural networks for wind speed forecasting. In *Proceedings of International Conference on Trends in Computational and Cognitive Engineering*, Mahendergarh, ed. P. Singh, R. K. Gupta, K. Ray, and A. Bandyopadhyay, Vol. 1169, pp. 79–94. Singapore: Springer. doi:10.1007/978-981-15-5414-8_6.

Benghanem, M., A. Mellit, and S. Alamri. 2009. Ann-based modelling and estimation of daily global solar radiation data: A case study. *Energy Conversion and Management* 50 (7):1644–55. doi:10.1016/j.enconman.2009.03.035.

Benmouiza, K., and A. Cheknane. 2019. Clustered anfis network using fuzzy c-means, subtractive clustering, and grid partitioning for hourly solar radiation forecasting. *Theoretical and Applied Climatology* 137 (1):31–43. doi:10.1007/s00704-018-2576-4.

Chaouachi, A., R. M. Kamel, and K. Nagasaka. 2010. Neural network ensemble-based solar power generation short-term forecasting. *Journal of Advanced Computational Intelligence and Intelligent Informatics* 14 (1):69–75. doi:10.20965/jaciii.2010.p0069.

David, M., F. Ramahatana, P. -J. Trombe, and P. Lauret. 2016. Probabilistic forecasting of the solar irradiance with recursive arma and garch models. *Solar Energy* 133:55–72. doi:10.1016/j.solener.2016.03.064.

Dinpashoh, Y., S. Jahanbakhsh-Asl, A. Rasouli, M. Foroughi, and V. Singh. 2019. Impact of climate change on potential evapotranspiration (case study: West and nw of Iran). *Theoretical and Applied Climatology* 136 (1):185–201. doi:10.1007/s00704-018-2462-0.

Feng, L., A. Lin, L. Wang, W. Qin, and W. Gong. 2018. Evaluation of sunshine-based models for predicting diffuse solar radiation in china. *Renewable and Sustainable Energy Reviews* 94:168–82. doi:10.1016/j.rser.2018.06.009.

Ghimire, S., R. C. Deo, N. Raj, and J. Mi. 2019. Deep solar radiation forecasting with convolutional neural network and long short-term memory network algorithms. *Applied Energy* 253:113541. doi:10.1016/j.apenergy.2019.113541.

Guermoui, M., F. Melgani, K. Gairaa, and M. L. Mekhalfi. 2020. A comprehensive review of hybrid models for solar radiation forecasting. *Journal of Cleaner Production* 258:120357. doi:10.1016/j.jclepro.2020.120357.

Hejase, H. A., M. H. Al-Shamisi, and A. H. Assi. 2014. Modeling of global horizontal irradiance in the united Arab emirates with artificial neural networks. *Energy* 77:542–52. doi:10.1016/j.energy.2014.09.064.

Huang, J., M. Korolkiewicz, M. Agrawal, and J. Boland. 2013. Forecasting solar radiation on an hourly time scale using a coupled autoregressive and dynamical system (cards) model. *Solar Energy* 87:136–49. doi:10.1016/j.solener.2012.10.012.

Jiang, Y. 2008. Prediction of monthly mean daily diffuse solar radiation using artificial neural networks and comparison with other empirical models. *Energy Policy* 36 (10):3833–37. doi:10.1016/j.enpol.2008.06.030.

Khan, K., and A. Sahai. 2012. A comparison of ba, ga, pso, bp and lm for training feed forward neural networks in e-learning context. *International Journal of Intelligent Systems & Applications* 4 (7):23. doi:10.5815/ijisa.2012.07.03.

Khare, V., S. Nema, and P. Baredar. 2016. Solar–wind hybrid renewable energy system: A review. *Renewable and Sustainable Energy Reviews* 58:23–33. doi:10.1016/j.rser.2015.12.223.

López, G., F. Batlles, and J. Tovar-Pescador. 2005. Selection of input parameters to model direct solar irradiance by using artificial neural networks. *Energy* 30 (9):1675–84. doi:10.1016/j.energy.2004.04.035.

Mandal, K., B. Bhattacharya, B. Tudu, and N. Chakraborty (2011). A novel population-based optimization algorithm for optimal distribution capacitor planning. In *2011 International Conference on Energy, Automation and Signal*, Bhubaneswar, India, pp. 1–6. IEEE. doi:10.1109/ICEAS.2011.6147075.

Marquez, R., and C. F. Coimbra. 2011. Forecasting of global and direct solar irradiance using stochastic learning methods, ground experiments and the nws database. *Solar Energy* 85 (5):746–56. doi:10.1016/j.solener.2011.01.007.

Mohanty, S., P. K. Patra, and S. S. Sahoo. 2016. Prediction and application of solar radiation with soft computing over traditional and conventional approach–a comprehensive review. *Renewable and Sustainable Energy Reviews* 56:778–96. doi:10.1016/j.rser.2015.11.078.

Ozgoren, M., M. Bilgili, and B. Sahin. 2012. Estimation of global solar radiation using ann over turkey. *Expert Systems with Applications* 39 (5):5043–51. doi:10.1016/j.eswa.2011.11.036.

Peled, A., and J. Appelbaum. 2013. Evaluation of solar radiation properties by statistical tools and wavelet analysis. *Renewable Energy* 59:30–38. doi:10.1016/j.renene.2013.03.019.

Pinker, R., R. Frouin, and Z. Li. 1995. A review of satellite methods to derive surface shortwave irradiance. *Remote Sensing of Environment* 51 (1):108–24. doi:10.1016/0034-4257(94)00069-Y.

Premalatha, N., and A. Valan Arasu. 2016. Prediction of solar radiation for solar systems by using ann models with different back propagation algorithms. *Journal of Applied Research and Technology* 14 (3):206–14. doi:10.1016/j.jart.2016.05.001.

Prescott, J. 1940. Evaporation from a water surface in relation to solar radiation. *Transactions of the Royal Society of South Australia* 46:114–18.

Rahmati, S. H. A., and M. Zandieh. 2012. A new biogeography-based optimization (bbo) algorithm for the flexible job shop scheduling problem. *International Journal of Advanced Manufacturing Technology* 58 (9):1115–29. doi:10.1007/s00170-011-3437-9.

Renno, C., F. Petito, and A. Gatto. 2016. Ann model for predicting the direct normal irradiance and the global radiation for a solar application to a residential building. *Journal of Cleaner Production* 135:1298–316. doi:10.1016/j.jclepro.2016.07.049.

Rensheng, C., E. Kang, Y. Jianping, L. Shihua, and Z. Wenzhi. 2004. Validation of five global radiation models with measured daily data in china. *Energy Conversion and Management 45* 45:1759–69. doi:10.1016/j.enconman.2003.09.019.

Ren, Y., P. Suganthan, and N. Srikanth. 2015. Ensemble methods for wind and solar power forecasting—a state-of-the-art review. *Renewable and Sustainable Energy Reviews* 50:82–91. doi:10.1016/j.rser.2015.04.081.

Samani, Z., A. S. Bawazir, M. Bleiweiss, R. Skaggs, and V. D. Tran. 2007. Estimating daily net radiation over vegetation canopy through remote sensing and climatic data. *Journal of Irrigation and Drainage Engineering* 133 (4):291–97. doi:10.1061/(ASCE)0733-9437(2007)133:4(291).

Sfetsos, A., and A. Coonick. 2000. Univariate and multivariate forecasting of hourly solar radiation with artificial intelligence techniques. *Solar Energy* 68 (2):169–78. doi:10.1016/S0038-092X(99)00064-X.

Shamshirband, S., K. Mohammadi, H. -L. Chen, G. N. Samy, D. Petković, and C. Ma. 2015. Daily global solar radiation prediction from air temperatures using kernel extreme learning machine: A case study for iran. *Journal of Atmospheric and Solar-Terrestrial Physics* 134:109–17. doi:10.1016/j.jastp.2015.09.014.

Shamshirband, S., K. Mohammadi, J. Piri, D. Petković, and A. Karim. 2016. Hybrid auto-regressive neural network model for estimating global solar radiation in Bandar Abbas, iran. *Environmental Earth Sciences* 75 (2):1–12. doi:10.1007/s12665-015-4970-x.

Sharma, V., D. Yang, W. Walsh, and T. Reindl. 2016. Short term solar irradiance forecasting using a mixed wavelet neural network. *Renewable Energy* 90:481–92. doi:10.1016/j.renene.2016.01.020.

Simon, D. 2008. Biogeography-based optimization. *IEEE Transactions on Evolutionary Computation* 12 (6):702–13. doi:10.1109/TEVC.2008.919004.

Singh, U., and T. S. Kamal. 2012. Concentric circular antenna array synthesis using biogeography based optimization. *Majlesi Journal of Electrical Engineering* 6 (7):822. doi:10.1049/iet-map.2011.0484.

Srivastava, S., and S. Lessmann. 2018. A comparative study of lstm neural networks in forecasting day-ahead global horizontal irradiance with satellite data. *Solar Energy* 162:232–47. doi:10.1016/j.solener.2018.01.005.

Voyant, C., G. Notton, S. Kalogirou, M. -L. Nivet, C. Paoli, F. Motte, and A. Fouilloy. 2017. Machine learning methods for solar radiation forecasting: A review. *Renewable Energy* 105:569–82. doi:10.1016/j.renene.2016.12.095.

Wu, G., Y. Liu, and T. Wang. 2007. Methods and strategy for modeling daily global solar radiation with measured meteorological data–a case study in Nanchang station, china. *Energy Conversion and Management* 48 (9):2447–52. doi:10.1016/j.enconman.2007.04.011.

Yadav, A. K., and S. Chandel. 2014. Solar radiation prediction using artificial neural network techniques: A review. *Renewable and Sustainable Energy Reviews* 33:772–81. doi:10.1016/j.rser.2013.08.055.

Yaghini, M., M. M. Khoshraftar, and M. Fallahi. 2013. A hybrid algorithm for artificial neural network training. *Engineering Applications of Artificial Intelligence* 26 (1):293–301. doi:10.1016/j.engappai.2012.01.023.

Zhao, N., X. Zeng, and S. Han. 2013. Solar radiation estimation using sunshine hour and air pollution index in china. *Energy Conversion and Management* 76:846–51. doi:10.1016/j.enconman.2013.08.037.